Species-Specific Voltage-Gating Properties of Connexin-45 Junctions Expressed in *Xenopus* Oocytes

Luis C. Barrio, Juan Capel, Jose A. Jarillo, Carmen Castro, and Ana Revilla
Departamento de Investigación, Neurología Experimental, Hospital Ramón y Cajal, Madrid 28034, Spain

ABSTRACT Gap junctions composed of connexin-45 (Cx45) homologs from four species, zebrafish, chicken, mouse, and human, were expressed in pairs of *Xenopus* oocytes. The macroscopic conductance (g_j) of all Cx45 junctions was modulated by transjunctional voltage (V_j) and by the inside-outside voltage (V_m), and the modulation was species specific. Although their gating characteristics varied in voltage sensitivity and kinetics, the four Cx45 junctions shared 1) maximum conductance at $V_j = 0$ and symmetrical g_j reduction in response to positive and negative V_j of low amplitude, with little residual conductance; and 2) g_j increases in response to simultaneous depolarization of the paired cells. The formation of hybrid channels, comprising Cx45 hemichannels from different species, allowed us to infer that two separate gates exist, one in each hemichannel, and that each Cx45 hemichannel is closed by the negativity of V_j on its cytoplasmic side. Interestingly, the V_m dependence of hybrid channels also suggests the presence of two gates in series, one V_m gate in each hemichannel. Thus the V_j and V_m dependence provides evidence that two independent voltage gates in each Cx45 hemichannel exist, reacting through specific voltage sensors and operating by different mechanisms, properties that have evolved divergently among species.

INTRODUCTION

Gap junctions provide a low-resistance pathway for ion flow and the passage of small molecules, mediating electrical and metabolic coupling between most vertebrate cell types. The gap-junctional channels are made up of protein subunits termed *connexins*. Each channel is a dodecamer composed of a hexamer of connexin subunits in each membrane. Multiple connexins have been cloned in rodents, and many homologs have been identified in other vertebrates (Bennett et al., 1995; Bruzzone et al., 1996). Expression of recombinant connexins in exogenous communication deficient cells or cells treated with antisense oligonucleotides to endogenous connexins has been used to determine the properties of intercellular channels formed by specific connexins; one important conclusion from these studies is that each connexin forms cell-to-cell channels with specific and somewhat divergent characteristics of gating by voltage (reviewed by Bennett and Verselis, 1992; Nicholson et al., 1993; White et al., 1995), cytoplasmic acidification (Werner et al., 1989; Liu et al., 1993; White et al., 1994; Hermans et al., 1995), or phosphorylation (reviewed by Bruzzone et al., 1996). Single-channel properties are also connexin specific: γ or single-channel conductance can vary between 30 pS and 300 pS, and there are multiple possible substates (e.g., Moreno et al., 1994; Veenstra et al., 1994a,b; Moreno et al., 1995; Trexler et al., 1996); differences in permeability to ions and small molecules can also be demonstrated (Veenstra et al., 1994a,b; Beblo et al., 1995; Elfgang et al., 1995). Much remains to be learned about the species-specific properties of junctional channels and about differences between orthologous connexins, i.e., connexins encoded by an ancestral gene with no intervening duplications. Cx45 was originally cloned from chick embryo (Beyer, 1990), and subsequent studies have identified homologous connexins in mouse (Henneman et al., 1992), dog (Kanter et al., 1992), human (Kanter et al., 1994), and, more recently, zebrafish (Essner et al., 1996). Cx45 is expressed in the embryos of several species, and its expression is regulated throughout development; it is widely distributed in adult tissues, including lung, heart, brain, intestine, and kidney (Beyer, 1990; Hennemann et al., 1992; Kanter et al., 1993; Chen et al., 1994).

The orthologs of Cx45 from all species show greater amino acid identity with each other than with other members of the connexin family, including those isoforms expressed in the same species. Mammalian Cx45 homologs from human, dog, and mouse have 97% identity with each other, and 83% with chicken (Fig. 1, *left*). Zebrafish Cx45 is the most divergent member of this subfamily, with only 54% amino acid identity with avian and 52% with mammalian Cx45 orthologs. As with other connexins, the degree of sequence conservation varies along the molecule; some domains are well conserved and others show marked divergences (Fig. 1, *right*). These divergent features may be neutral or may confer functional differences. Some differences in voltage dependence were reported between chicken, dog, and human Cx45 channels expressed either endogenously (HCx45, Moreno et al., 1995) as well as exogenously in transfected cells (ChCx45, Veenstra et al., 1992) or in the *Xenopus* oocyte system (ChCx45, Barrio et al., 1995b; DCx45, Steiner and Ebihara, 1996). These differences may be due to differences in the cellular environ-

Received for publication 19 December 1996 and in final form 17 April 1997.

Address reprint requests to Dr. Luis C. Barrio, Departamento de Investigación, Servicio de Neurología Experimental, Hospital "Ramón y Cajal," Carretera de Colmenar Km 9.1, 28034-Madrid, Spain. Tel.: 34-1-336.8320; Fax: 34-1-336.9816; E-mail:luis.c.barrio@hrc.es.

0006-3495/97/08/757/13 $2.00

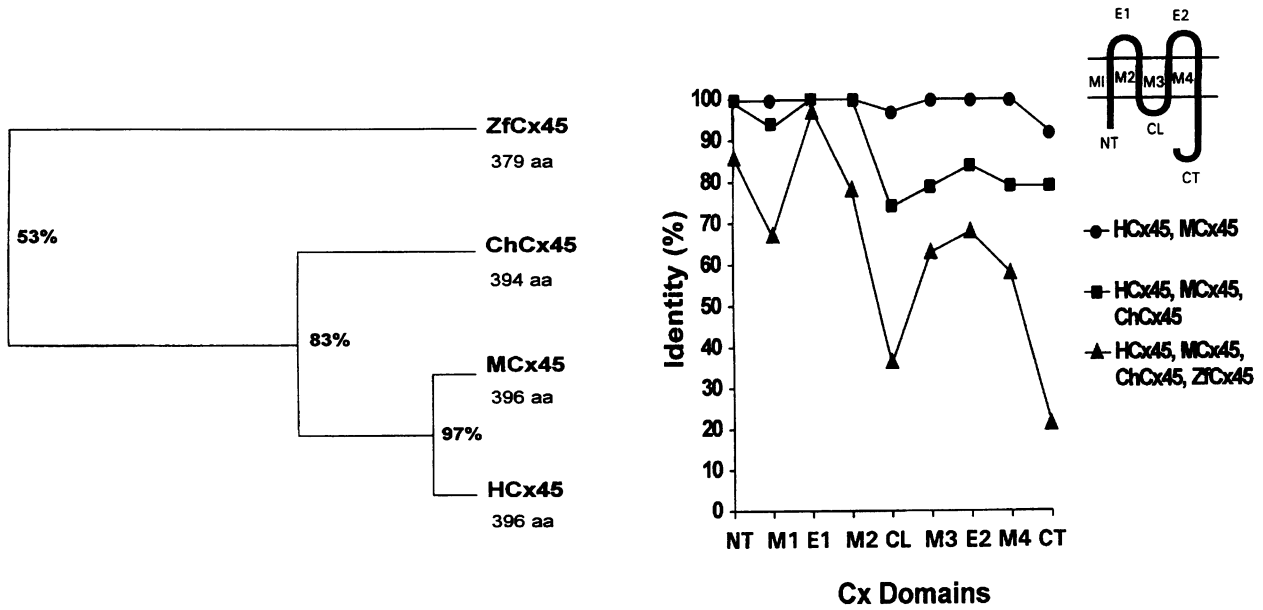

FIGURE 1 Phylogenetic tree of Cx45 orthologs and the distribution of amino acid identity by connexin domains. (*Left*) Cx45 tree, built by divergence analysis using the Clustal analysis (Higgins and Sharp, 1988), shows the branches and the relative distances among zebrafish, chicken, mouse, and human connexins. The length of the coding sequence and the percentage of amino acid identity in all species are indicated. (*Right*) Distribution of amino acid identity within domains of the molecule, according to the accepted topology of connexins (Bennett et al., 1991). The percentage identity is defined as 100 times the ratio of the number of identical residues divided by the largest number of residues in that domain. There are nine principal domains (*inset*): four membrane-spanning regions (M1–M4); two extracellular loops (E1, E2); a cytoplasmic loop (CL) connecting M2 and M3; and the N-terminus (NT) and carboxyl terminus (CT) on the cytoplasmic side. Divergences are nonuniformly distributed; in human and mouse, identity is complete in all domains except CL and CT. Between mammalian and avian, the identity is complete in NT, E1, and M2, and decreases in M1 and from CL to CT. Among all species, the identity is still high (>85%) in NT and E1, moderate (60–80%) in M1–M4 and E2, and low (20–40%) in CL and CT.

ment or to differences in their sequences. In the present investigation, we compared the voltage gating of macroscopic conductance of Cx45 channels from four species, zebrafish, chicken, mouse, and human, all expressed in the same environment, paired *Xenopus* oocytes. We found that each kind of Cx45 channel had unique voltage-gating phenotypes, although the different kinds of channels shared some features in common. As a consequence of the peculiar architecture of cell-to-cell channels (i.e., they are formed by two hemichannels or connexons, each spanning a plasma membrane and meeting in the intercellular gap), they are under the influence of two voltage differences, i.e., the voltage between the two cell interiors or transjunctional voltage (V_j), and that between the cell interiors and the extracellular spaces or membrane potential (V_m). Although Cx45 from all species formed channels whose conductance was dependent on transjunctional voltage (V_j) and on inside-outside voltage (V_m), they varied in voltage sensitivity and in kinetics. We interpret our data as indicating that there are two separate gates in each hemichannel, one specifically sensing V_j, and one sensing V_m. This independence was inferred from the comparison of voltage dependence in homotypic and heterotypic combinations. Furthermore, the gating properties associated with each kind of voltage sensor in the Cx45 channels of fish, avian, and two mammal species, mouse and human, have diverged during vertebrate evolution.

MATERIALS AND METHODS

Preparation of cRNAs

Zebrafish Cx45 (ZfCx45) was cloned using a polymerase chain reaction approach with degenerate oligonucleotides. The amplified cDNA fragments were used to screen a gastrula-stage lambda ZAP II (Stratagene) cDNA library (kindly provided by Dr. Grunwald), and three full-length cDNA clones were obtained (GeneBank accession number X96-712). A 2-kb cDNA fragment, containing an open reading frame of 379 amino acids that encodes a protein of 43.4 kDa, was inserted in pBlueScript vector (Stratagene), linearized with *Spe*I, and sense transcribed with T7 polymerase. A pBlueScript vector containing the chicken Cx45 (ChCx45) (clone CE15D; Beyer, 1990) was linearized with *Sma*I for in vitro transcription of sense cRNA with T3 RNA polymerase. The cRNAs of mouse Cx45 (MCx45) (Hennemann et al., 1992) and human Cx45 (HCx45) (Kanter et al., 1994) were transcribed with T7 polymerase after linearization with *Not*I and *Eco*RI of the respective pBlueScript vectors.

All cRNA synthesis was performed under standard reaction conditions (protocol and reagents from Promega) in the presence of the cap analog $m^7G(5')ppp(5')G$ (Boehringer Mannheim). After DNase digestion and purification, cRNAs were quantified by absorbance (260 nm), and the proportion of full-length transcripts (>90%) was checked on a 1% agarose gel stained with ethidium bromide.

Expression in pairs of *Xenopus* oocytes

Oocytes were removed from ovaries of *Xenopus laevis* frogs (purchased from Nasco) under anesthesia (3-aminobenzoic acid ethyl ester, 2 g/l; Sigma) and treated for 1 h with collagenase (type D, 1 mg/ml; Boehringer Mannheim) in ND96 without calcium (in mM: 96 NaCl, 2 KCl, 1 $MgCl_2$,

and 5 HEPES, supplemented with 2.5 pyruvate and penicillin/streptomycin; pH 7.45). Oocytes (stage V and VI) were manually defolliculated and, after overnight recovery in ND96 with 1.8 mM $CaCl_2$, coinjected with an antisense oligonucleotide directed against *Xenopus* Cx38 mRNA to block endogenous expression (10 ng/oocyte; Barrio et al., 1991), and with the in vitro transcribed cRNA of zebrafish, chicken, mouse or human Cx45 (0.1–0.5 $\mu g/\mu l$; 50 nl/oocyte). Vitelline membranes were removed in hypertonic solution (in mM: 200 K-aspartate, 20 KCl, 1 $MgCl_2$, 1 EGTA, 10 HEPES, pH 7.45) before pairing.

Measurement of junctional conductance

Pairs injected with four kinds of Cx45 cRNAs were recorded after 24–72 h in ND96 (in mM: 96 NaCl, 2 KCl, 1 $MgCl_2$, 1.8 $CaCl_2$, 5 HEPES, pH 7.45), using microelectrodes of 0.5–1 MΩ filled with 2 M KCl, 10 mM EGTA, and 10 mM HEPES (pH 7.20). The dual voltage-clamp technique impaling each cell of the pair with two microelectrodes connected to an independent amplifier (TEV-200; Dagan) was used to measure macroscopic junctional conductance (g_j). The procedure to measure g_j was as follows, where V_1, I_1, V_2, and I_2 are voltages and currents, with the holding current subtracted, in oocytes 1 and 2, respectively. First, both oocytes were clamped at the same holding potential (V_m, e.g., −40 mV), then V_j = 0, because $V_j = V_1 - V_2$. To explore the influence of V_j on junctional conductance, voltage steps of positive and negative polarities were applied in oocyte 1, defining positive V_j as greater relative positivity in oocyte 1. In this procedure the currents injected in oocyte 2 (I_2) to hold its potential constant were equal in magnitude to and opposite in sign from the currents flowing through the junctional channels ($I_j = -I_2$), and the g_j was calculated as I_j/V_j. The stability of junctional conductance was controlled by applying a small and brief prepulse just before each V_j step during the recording period. The V_m dependence of g_j was explored by equal displacement of holding potentials in both cells of the pair, and the g_j was monitored by application of test V_j pulses too small and brief to induce g_j changes. Stimulation and data collection were performed using a PC-AT computer, a Digidata 1200-A interface, and pCLAMP software (Axon), and junctional currents were low-pass filtered at 1 KHz. The initial junctional conductance (g_{j0}) was measured with 0.5 ms/bin resolution, as soon as the full clamping voltage was reached, 1–5 ms after the voltage onset. Steady-state g_j values (g_{jss}) were obtained by using pulses of sufficient duration: 5 s for ZfCx45 and ChCx45 junctions, whereas pulses of 10 s were required in the case of MCx45 and HCx45 junctions.

Junctional conductance and kinetics modeling

The common method of evaluating the voltage dependence of gap junctions is to fit the macroscopic junctional conductance/voltage relationship to a Boltzmann relation of the form (Spray et al., 1981)

$$G_{jss} = \{(G_{jmax} - G_{jmin})/(1 + \exp[A(V_j - V_0)])\} + G_{jmin},$$

which applies to a two-state system with the energy difference between states linearly dependent on voltage. Although not all Cx45 channels may meet these assumptions (see Results), this analysis still provides useful parameters for comparing the behavior of different Cx45 channels. The G_{jmax} is the maximum conductance, G_{jmin} is the residual conductance at large V_j or voltage-insensitive component of the conductance, V_0 is the transjunctional voltage at which $G_{jss} = (G_{jmax} - G_{jmin})/2$, A ($A = nq/kT$) is a constant that expresses the voltage sensitivity in terms of gating charge as the equivalent number (n) of electron charges (q) moving through the entire membrane voltage, and kT has its usual significance. Steady-state g_j (G_{jss}) was normalized relative to the g_j value for brief V_j prepulses (10 mV) and plotted versus voltage. The averaged G_{jss}/V_j relationships of homotypic junctions were well described by a single Boltzmann relation for each polarity of V_j, based on the assumption that each polarity of V_j affected a single gap junction hemichannel (see Results). The averaged steady-state G_j/V_m relationships of homotypic junctions after normalization relative to g_j at V_m = −100 mV were fitted to a single and to squared Boltzmann relations according to the assumption of a model of a unique gate and of two independent gates in series, one per hemichannel (Verselis et al., 1991). The fitting strategy could not resolve the most appropriate of the alternative models, because the data were well described by both types of Boltzmann relations. This limitation could be accounted for by the smooth g_j changes within the range of V_m used. However, the appropriateness of a model with two independent gates in series could be inferred from the gating properties of hybrid ZfCx45-MCx45 junctions, because the V_m dependence was intermediate to those exhibited by their parent homomeric channels, which suggests the presence of one V_m gate in each hemichannel. Fits were made by treating G_{jmax}, G_{jmin}, A, and V_0 as free parameters, and the best values of constants were obtained by applying an iterative procedure of fitting to minimize the least-squares error between data and the calculated fit point (SigmaPlot; Jandel Scientific). The least-squares fit procedure provided values of G_{jmax} and G_{jmin} extrapolated from the experimental data.

The time courses of g_j transitions were fitted to exponential relations with $R < 0.999$, using Clampfit (pCLAMP; Axon). The relationships between the voltage, time constant, and steady-state conductance were modeled according to a two-state Boltzmann system (Harris et al., 1981). The rate constants of transitions between states of high and low conductances were calculated from experimental time constants (τ) and G_{jss} as $\alpha = G_j/\tau$ and $\beta = (1 - G_j)/\tau$, where $G_j = G_{jss} - G_{jmin}$, i.e., the voltage-sensitive component of conductance. The parameters of voltage dependence of the rate constants were obtained from the best fit of data to $\alpha = \lambda \exp[-A_\alpha(V_j - V_0)]$, $\beta = \lambda \exp[A_\beta(V_j - V_0)]$, where A_β and A_α express voltage sensitivities of closing and opening rates, V_0 is the voltage at half-inactivation conductance, and λ is the rate for which $\alpha = \beta$, reached at $V_j = V_0$. Then the voltage-dependent curves of time constants were calculated as $\tau = 1/(\alpha + \beta)$. The same procedure was followed to obtain the parameters of V_m dependence of the rates and time constants.

RESULTS

Pairs of *Xenopus* oocytes, microinjected with Cx45 cRNAs of zebrafish, chick, mouse, or human, all developed high levels of electrical coupling, indicating that they were all able to form functional gap-junction channels with similar efficacy. The macroscopic conductance (g_j) of all of the Cx45 junctions was dependent on both transjunctional and inside-outside voltages (V_j and V_m). The voltage dependence was more marked in pairs with lower values of g_j (<15–20 μS), but was still detectable in pairs with the largest g_j values (40–100 μS). This apparent reduction in voltage sensitivity, combined with characteristic changes in the kinetics of g_j, may reflect an increase in access resistance to the tightly packed gap junction channels as more channels were incorporated into junctional plaques (Wilders and Jongsma, 1992). To avoid this limitation, the effects of V_j and V_m were characterized in pairs with g_j between 0.5 and 15 μS.

V_j dependence

The responses of the four types of Cx45 channels to V_j between ±100 mV are illustrated in Fig. 2. The junctional conductance of all types of Cx45 channels had the following characteristics: 1) a maximum g_j (g_{jmax}) at V_j = 0; 2) a symmetrical g_j reduction in response to positive and negative V_j, even of low amplitude, with progressively larger and faster reductions at larger V_j; and 3) a low minimum conductance, $g_{jmin} < 0.05–0.11\ g_{jmax}$ at large V_j. Differences

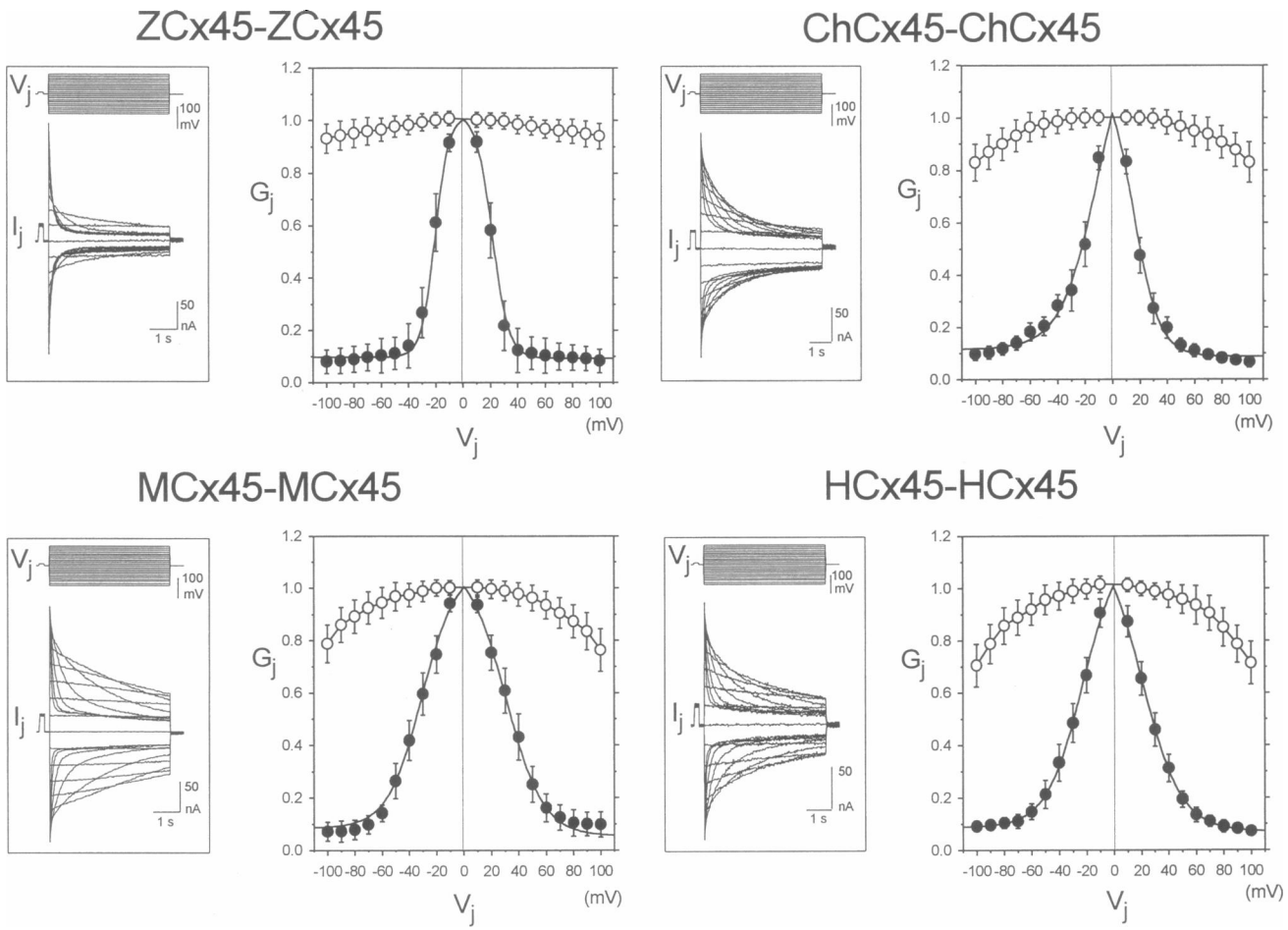

FIGURE 2 Transjunctional voltage dependence of zebrafish (ZfCx45), chicken (ChCx45), mouse (MCx45), and human Cx45 (HCx45) gap junctions. (*Left*) Sample records of junctional currents (I_j) evoked by voltage steps (V_j) in pairs expressing the four kinds of homomeric Cx45 channels (V_j = ±100 mV range, increments of 10 mV, durations of 5 s). Positive V_j and I_j elicited were displayed upward. Progressively larger and faster decreases in I_j were induced as V_j increased. (*Right*) Graphs of initial (○) and steady-state (●) G_j/V_j relations (means ± SD, n = 10 for each type of junction); g_j was normalized to the value at the V_j prepulse (10 mV). Curves are described by the single Boltzmann relation for each V_j polarity, which required species-specific parameters (Table 1).

between the different Cx45 channels were quantified in terms of the initial and steady-state G_j/V_j relationships, being the g_j's of the four types of junctions normalized relative to their values measured with small prepulses, too brief to affect coupling. In contrast to the ohmic behavior of the initial g_j exhibited by zebrafish Cx45 channels, the g_{jo} values of avian and mammalian Cx45 channels diminished progressively as larger V_j were applied. These reductions suggest the existence of a very fast closing process, faster than our clamping time resolution (1–5 ms), or, alternatively, they may reflect single-channel rectification, as in Cx46 hemichannels (Trexler et al., 1996) and hybrid Cx26-Cx32 channels (Bukauskas et al., 1995). The degree of rectification at the macroscopic level increased progressively from teleost to mammal, and it was most pronounced in human Cx45 channels, where g_{jo} was reduced by 20–30% at V_j = ±100 mV.

There were also differences between the steady-state G_j/V_j relationships of the four types of Cx45 junctions. The steady-state g_j values reached in response to V_j of each polarity were well described by symmetrical single Boltzmann relations with species-specific values for half-inactivation voltage (V_0) and voltage sensitivity (A) (Table 1). The conductance of ZfCx45 junctions was the most voltage sensitive, with A = 0.17–0.19 mV^{-1} or a calculated gating charge of 4.3–4.9, whereas avian and mammalian Cx45 channels had similar sensitivities to V_j, with A = 0.07–0.10 mV^{-1} or a gating charge of 2.00–2.02. The V_0 values also varied; V_0 was close to ±10 mV for chick Cx45 channels, was about ±20 mV for zebrafish and human, and was ±30 mV for mouse. The theoretical fits estimated G_{jmin} values close to experimental data at the larger V_j values explored, and were similar for the different Cx45 junctions (0.11–0.5). In contrast, the calculated G_{jmax} values were greater than experimental g_{jmax} obtained at V_j = 0, with the exception of the ZfCx45 junction: G_{jmax} values were 1.34–1.19 for chick, 1.21–1.16 for human, and 1.18–1.10 for mouse Cx45 junctions. The extrapolated values of $G_{jmax} > 1$

TABLE 1 Boltzmann parameters of transjunctional voltage dependence (V_j) for homotypic zebrafish (ZfCx45), chicken (ChCx45), mouse (MCx45), and human Cx45 (HCx45) junctions and for heterotypic ZfCx45-MCx45 junctions expressed in *Xenopus* oocytes*

	V_j (−)					V_j (+)							
	A	n		G_{jmax}	G_{jmin}	A	n	V_0	G_{jmax}	G_{jmin}	A_β	A_α	λ
ZfCx45-ZfCx45	0.19	4.90	20.6	1.02	0.10	0.17	4.29	21.3	1.02	0.09	0.091	0.084	0.238
ChCx45-ChCx45	0.07	2.00	10.4	1.34	0.11	0.10	2.53	12.7	1.19	0.09	0.056	0.025	0.130
MCx45-MCx45	0.08	2.02	30.8	1.18	0.08	0.07	1.77	30.7	1.10	0.05	0.062	0.028	0.079
HCx45-HCx45	0.08	2.02	22.8	1.16	0.08	0.07	1.77	20.7	1.21	0.07	0.047	0.042	0.127
ZfCx45-MCx45	0.23	5.80	20.7	1.05	0.13	0.07	1.77	22.6	1.13	0.04			

* The junctional conductance for each V_j polarity was described by a single Boltzmann relation, based on the assumption that each polarity of V_j affected a single gap junction hemichannel. A, voltage sensitivity (mV^{-1}); n, calculated gating charge at 20°C; V_0, voltage value of half-inactivation in g_j (mV); G_{jmax}, theoretical maximum conductance extrapolated from the data; G_{jmin}, extrapolated values of residual conductance, i.e., voltage-insensitive component. In the case of heterotypic ZfCx45-MCx45 junctions, negative and positive V_j are defined as relative negativity in the cytoplasmic side of ZfCx45 and MCx45 hemichannels, respectively. A_β and A_α are the voltage sensitivities (mV^{-1}) of closing and opening rate constants, and λ is a constant (s^{-1}) calculated as described in Materials and Methods.

indicate that higher values of conductance would be reached with the opposite polarity of V_j than that which induces closing. In the case of apposed hemichannels, a greater conductance was precluded by the closure of the other hemichannel.

The slow transitions from high to low conductance were symmetrical for positive and negative V_j and exponential in time course with faster time constants as V_j increased (Figs. 2 and 3). A second decay component of low amplitude and slower time course became apparent at $V_j > 50-60$ mV (Fig. 3, *insets*). Differences in kinetics among types of Cx45 junctions involved differences in time constants and relative amplitudes of major and minor components. Representative examples of the time constants of the main component (τ_1) of g_j decay during V_j pulses of 50 mV were 224 ms for ZfCx45, 1433 ms for ChCx45, 3117 ms for MCx45, and

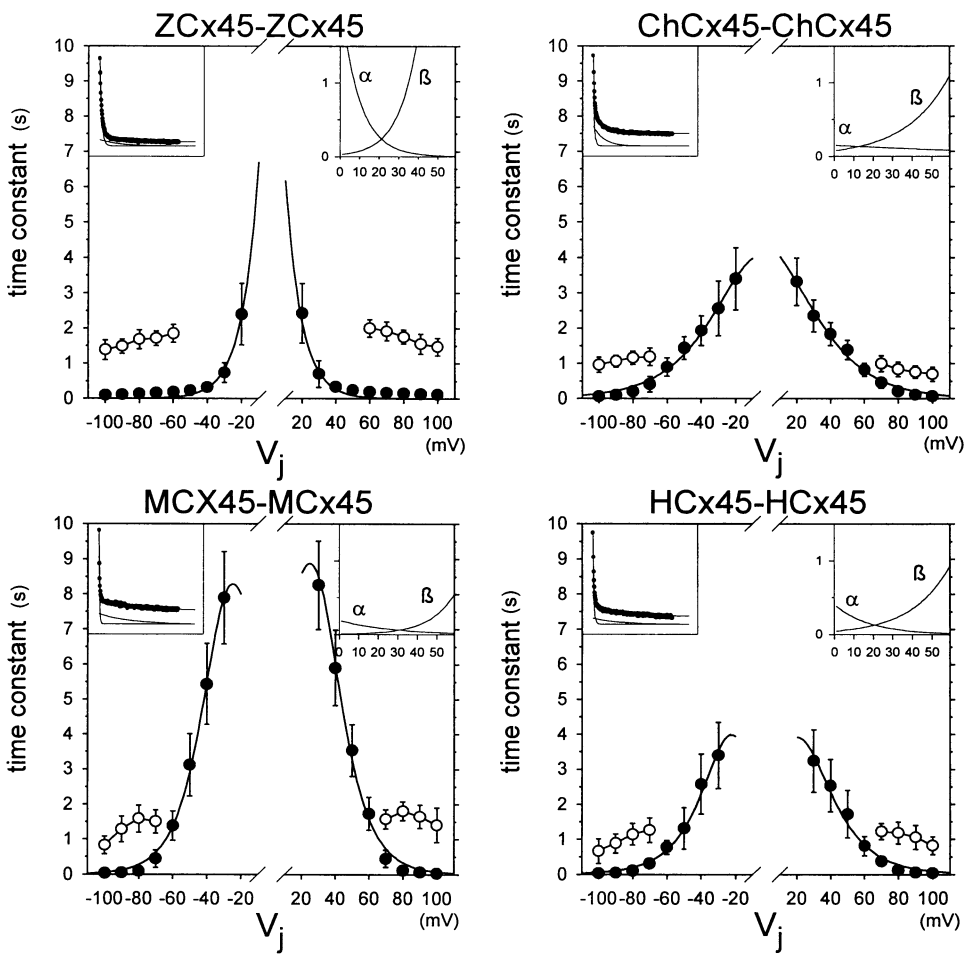

FIGURE 3 Kinetics of V_j dependence; experimental and calculated time and rate constants. The time courses of V_j-induced g_j transitions followed biexponential relations, with a fast component of major amplitude and a minor slower component at $V_j > 50-60$ mV superimposed on a residual conductance, g_{jmin} (*left insets*, for $V_j = +100$ mV). Time constants (τ) of major (●) and minor (○) components were plotted versus positive and negative V_j (means ± SD, $n = 6$ for each type of junctions). (*Right insets*) Opening and closing rate constants (α and β) of the main component of g_j decay, calculated from experimental τ's and junctional conductance values, were fitted to $\alpha = \lambda \exp[-A_\alpha(V_j - V_0)]$ and $\beta = \lambda \exp[A_\beta(V_j - V_0)]$ with species-specific parameters (Table 1). Time constants were then calculated as $\tau = 1/(\alpha + \beta)$ (*continuous curve*).

1309 for HCx45. For larger pulses of 100 mV, the mean values of the time constants of fast and slower components were τ_1 = 92 ms and τ_2 = 1278 ms, with a ratio of amplitudes of major and minor components of 13-fold for ZfCx45; τ_1 = 58 ms, τ_2 = 954 ms, and 4-fold for ChCx45; τ_1 = 28 ms, τ_2 = 826 ms, and 8-fold for MCx45, and τ_1 = 34 ms, τ_2 = 664 ms, and 6-fold for HCx45 junctions.

Thus the results demonstrate that the conductance of Cx45 junctions of the four species, zebrafish, chicken, mouse, and human, is strongly dependent on transjunctional voltage with species-specific parameters of voltage sensitivity and kinetics.

Inside-outside voltage dependence

The influence of inside-outside voltage (V_m) on junctional conductance was explored independently of V_j by displacing the holding potentials equally while monitoring the junctional conductance with test V_j pulses that were too small and brief to affect coupling (Fig. 4, *left*). During depolarizing pulses, g_j of the four types of Cx45 junctions increased until a new steady-state value was reached with higher conductances at more depolarized membrane potentials. g_j decreased to its previous value when V_m was returned to the initial hyperpolarized holding potential (−100

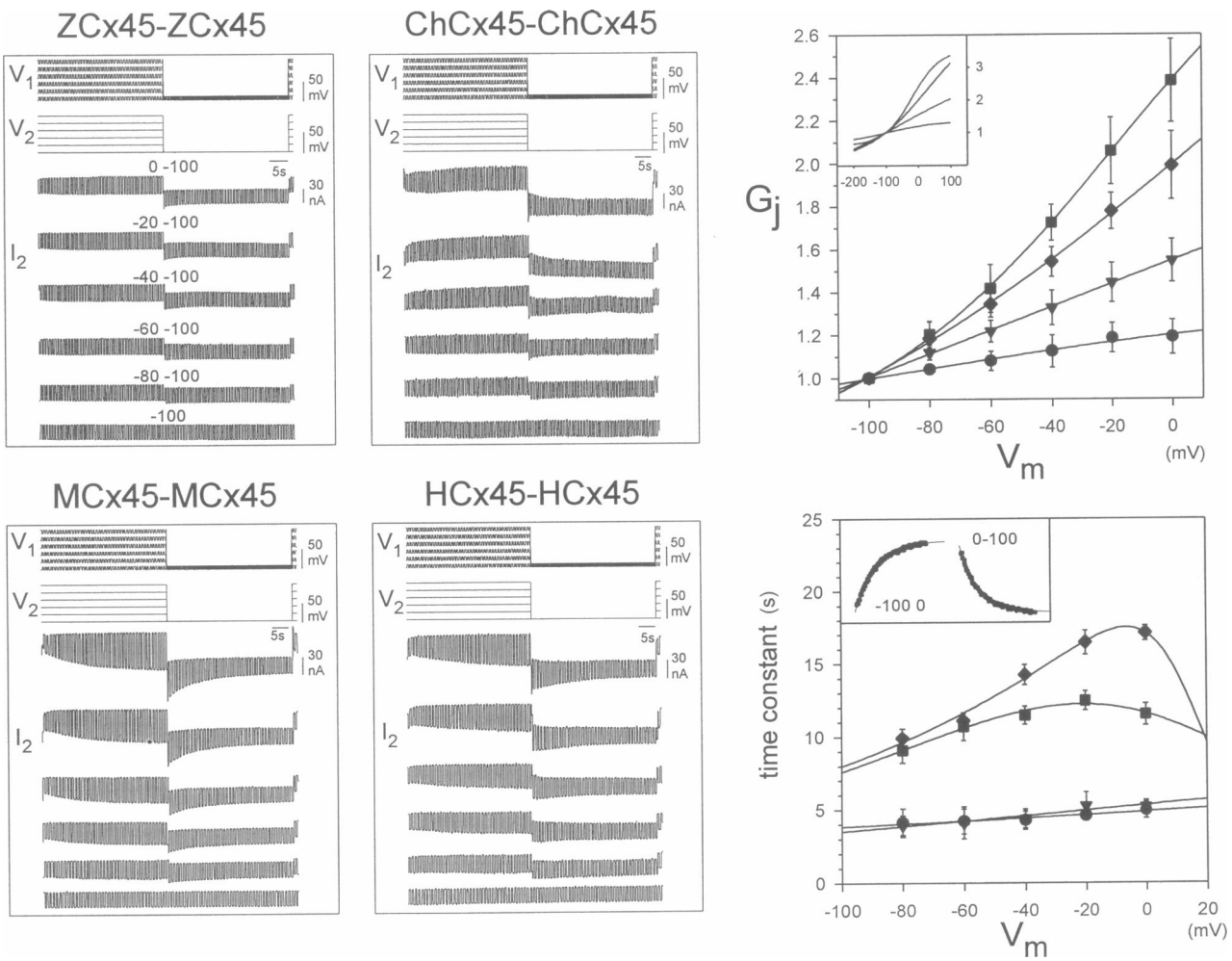

FIGURE 4 Inside-outside voltage dependence of zebrafish (ZfCx45), chicken (ChCx45), mouse (MCx45), and human Cx45 (HCx45) junctions. (*Left panels*) Sample records of currents (I_2) in response to equal displacements of potential in both cells of a pair, V_1 and V_2, stepping from a holding potential of −100 to 0 mV by increments of 20 mV and returning to −100 mV (40-s pulse durations and intervals). g_j was measured by applying small and brief V_j pulses in oocyte 1 to cause pulses in I_2 proportional to g_j (±10 mV, 500 ms, 1 Hz). For all four types of junction, g_j increased with increasing depolarization of V_m, and decreased to the control value when V_m was returned to −100 mV. (*Right upper graphs*) Steady-state G_j/V_m relationships (means ± SD, n = 6 for each type of junction) of zebrafish (●), chicken (▼), mouse (♦), and human (■). G_{jss} is the value normalized to that at V_m = −100 mV. The smooth curves were described by squared Bolztmann relations (*inset*), according to a model of two independent gates in series (see Materials and Methods), requiring species-specific parameters (Table 2). Sensitivity to V_m was weakest for ZfCx45, greater for ChCx45 and HCx45, and greatest for MCx45. (*Right bottom graphs*) Kinetics of V_m-induced g_j changes. Time courses of increasing and decreasing g_j's were well fitted by single exponentials (*insets*); the time constants were plotted as a function of V_m (means ± SD, n = 6 for each type of junction) and represented as $\tau = 1/(\alpha + \beta)$ (*continuous curve*).

mV). The magnitude and time course of V_m-induced increases in g_j varied markedly among the different types of Cx45 junction. V_m had little effect on ZfCx45 junctions, increasing g_j by less than 10–15% for depolarizations from −100 to 0 mV. This amount of depolarization of V_m had more effect on the other Cx45 junctions, increasing g_j of chicken, human, and mouse Cx45 junctions by 1.5-, 2-, and 2.5-fold, respectively. The steady-state G_j/V_m relations were well described by the product of two Boltzmann relations, a calculation based on the assumption that there are two independent gates in series, one per hemichannel (Fig. 4, *right upper*), which is validated by the effect of V_m on hybrid ZfCx45-MCx45 junctions (see below). The parameters of voltage sensitivity (A) and half-inactivation voltage (V_0) were species-specific (Table 2). V_m sensitivity increased from fish to avian, and from avian to mammalian. The mouse Cx45 junction was the most V_m sensitive, with $A = 0.021\ mV^{-1}$ or a 0.53 gating charge. Thus the V_m sensitivity of MCx45 junctions was about fivefold weaker than the V_j sensitivity.

The g_j transitions for depolarizing and hyperpolarizing V_m were well fit by single exponential functions with time constants of several seconds (Fig. 4; *right bottom*). The time constants were shorter at more hyperpolarized V_m and were independent of previous history. These kinetic data are consistent with a two-state model with energy differences between states proportional to voltage. The kinetic properties were also species-specific, because ZfCx45 and ChCx45 junctions showed similar and shorter time constants, whereas HCx45 junctions exhibited the longest time constants and MCx45 junctions showed intermediate values.

Thus the four kinds of Cx45 junctions were all sensitive to both V_j and V_m, with differences in the degree of influence at each voltage. Zebrafish Cx45 junctions were mainly modulated by V_j, whereas avian and mammalian Cx45 junctions combined strong V_j dependence with weak to moderate V_m. V_j dependence was more voltage sensitive ($A = 0.07–0.19\ mV^{-1}$ or $n = 2.0–4.9$) and had faster and more complex kinetics; V_m dependence was less voltage sensitive ($A = 0.002–0.021\ mV^{-1}$ or $n = 0.05–0.53$) and had slower and simple first-order kinetics.

V_j and V_m dependence of hybrid Cx45 junctions

When oocytes expressing Cx45 of different species were paired, coupling developed between them, demonstrating that Cx45 orthologs are able to form heterotypic junctions. The effects of V_j and V_m on g_j of ZfCx45-MCx45 junctions are illustrated in Figs. 5 and 6. In agreement with the heterotypic nature of the junction, junctional currents in response to positive and negative V_j pulses were asymmetrical (Fig. 5). V_j pulses negative in the oocyte expressing ZfCx45 induced junctional currents equal to those induced by equivalent positive pulses in the oocyte expressing MCx45 (Fig. 5, *left*, downward currents in the upper records, upward currents in the lower records). These responses resembled those induced by V_j pulses in homotypic ZfCx45 junctions (Fig. 2, ZfCx45-ZfCx45). Similarly, responses to V_j negative on the MCx45 side or positive on the ZfCx45 side resembled those of homomeric MCx45 junctions (Fig. 2, MCx45-MCx45). These data suggest that 1) there are two independent V_j gates, one in the ZfCx45 hemichannel and one in the MCx45 hemichannel; 2) each closes in response to V_j negative on its cytoplasmic side; and 3) the characteristics of V_j gating by each hemichannel are little affected by association with the other hemichannel. The initial and steady-state G_j/V_j relations of ZfCx45-MCx45 junctions for each polarity were plotted with the more similar G_j/V_j relation of the homomeric junctions, i.e., the MCx45 relation for relative positivity on the ZfCx45 side and the ZfCx45 relation for relative negativity on the ZfCx45 side (Fig. 5, *upper right*). The initial G_j/V_j relation for ZfCx45-MCx45 junctions showed a weak and asymmetrical rectification for both polarities of V_j, with slightly lower g_{j0} values for relative negativity of V_j on the MCx45 side. Because the g_{j0} of homotypic ZfCx45 junctions did not show fast rectification, the observed rectification in the heterotypic junctions may be contributed by the MCx45 hemichannels responding to both polarities of V_j. Apposing two identical hemichannels in general tends to preclude asymmetries in g_{j0} of this kind. The steady-state G_j/V_j relations were also asymmetrical, and the maximum g_j value was shifted slightly from $V_j = 0$ to a small relative nega-

TABLE 2 Boltzmann parameters of inside-outside voltage dependence (V_m) for homotypic zebrafish (ZfCx45), chicken (ChCx45), mouse (MCx45), and human Cx45 (HCx45) junctions and for heterotypic ZfCx45-MCx45 junctions expressed in *Xenopus* oocytes*

	A	n	V_0	G_{jmax}	G_{jmin}
ZfCx45-ZfCx45	0.002	0.05	−126	1.21	0.97
ChCx45-ChCx45	0.006	0.15	−98	1.73	0.03
MCx45-MCx45	0.021	0.53	−35	2.30	0.78
HCx45-HCx45	0.007	0.20	−28	2.89	0.28
ZfCx45-MCx45*	0.018	0.45	−18	2.26	0.82

* Junctional conductance of homotypic junctions was described by a squared Boltzmann relation, assuming the model of two independent gates in series, one per hemichannel.

* The fit of the conductance of ZfCx45-MCx45 junctions to a single Boltzmann where the parameters were close to those calculated for each hemichannel of homotypic MCx45 junctions confirmed the appropriateness of the model of two independent gates. The values of steady-state conductance were normalized to that at $V_m = -100$ mV. A, Voltage sensitivity (mV^{-1}); n, calculated gating charge at 20°C; V_0, half-g_j inactivation voltage (mV); G_{jmax}, estimated maximum conductance extrapolated from data; G_{jmin}, estimated residual conductance, i.e., voltage-insensitive component.

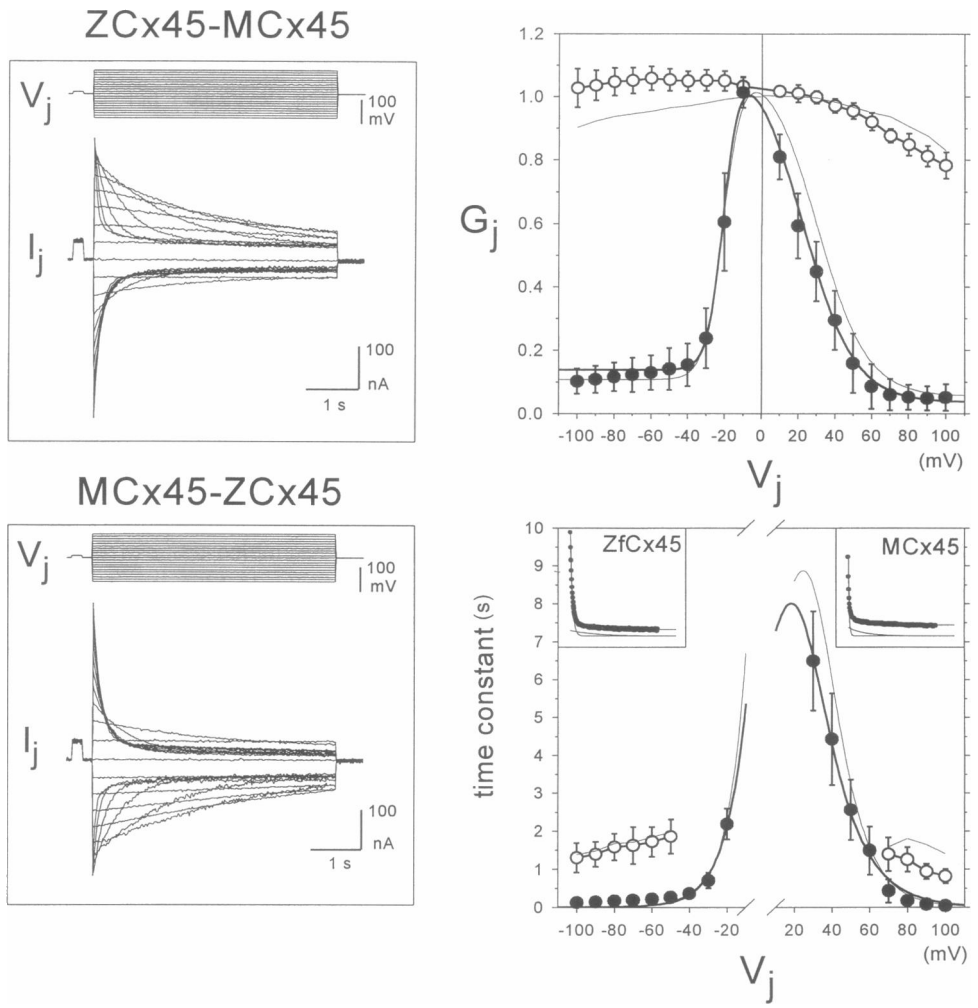

FIGURE 5 Transjunctional voltage dependence of heterotypic ZfCx45-MCx45 junctions. (*Left*) Junctional currents (I_j) elicited by the same transjunctional voltage (V_j) protocol ($V_j = \pm 100$ mV range, increments of 10 mV and durations of 5 s) applied in the oocyte expressing ZfCx45 (*upper*) and MCx45 (*bottom*). Positive and negative V_j polarities are defined as relative depolarizations and hyperpolarizations of the cell when the pulses were applied and induced upward and downward I_j, respectively. (*Upper right*) Graph of initial (○) and steady-state (●) G_j/V_j relations (mean ± SD, $n = 6$ pairs). G_{jss}/V_j for each polarity was described by a single Boltzmann relation (*continuous curves*). The averaged G_{jo}/V_j relationship and the G_{jss}/V_j curve calculated as the product of single Boltzmann relations fitting each hemichannel of homotypic ZfCx45 and MCx45 junctions were superimposed. (*Bottom*) Dependence of time constants on V_j (mean ± SD, $n = 6$ pairs). g_j transients were fitted by biexponential relation (*insets*; ZfCx45 *left*, MCx45 *right*) and the calculated time constants of the major component plotted as a function of V_j of heterotypic and homotypic junctions (*curves*). In right graphs, positive V_j corresponds to relative positivity in the oocyte expressing ZfCx45 and relative negativity on the MCx45 side.

tivity on the ZfCx45 side. The steady-state G_j/V_j relation for positive and negative V_j polarities was fit well by the product of those single Boltzmann relations calculated for negative polarity of V_j in the homomeric parent junctions (Fig. 1 and Table 1), in accordance with a model of gating with two independent gates in series. However, two minor deviations of this model were found, because the experimental V_j value at maximum g_j was somewhat greater and the voltage value of half-g_j inactivation for relative negativity on the MCx45 side was reduced from 30 to 20 mV without changes in gating charge (Table 1).

The kinetics of V_j-induced g_j transitions for relative negativity on the ZfCx45 side were identical to those observed in ZfCx45 homotypic junctions (Fig. 5; *right bottom*). For relative negativity on the MCx45 side, g_j decayed as a single exponential at lower V_j and with the addition of a small slower component at higher V_j (>50–60 mV), as in MCx45 homotypic junctions. However, the relation between time constant and voltage was shifted toward somewhat smaller voltage. These changes in kinetics were consistent with the small shift of the G_j/V_j relationship toward less negative V_j values on the MCx45 side. In summary, the V_j dependence of the heterotypic junctions could be accounted for largely in terms of the gating properties attributable to each hemichannel in their homomeric junctions. Yet there were small changes that would not be predicted from the simple assumption of complete independence of the apposed hemichannels.

We have also analyzed the V_m dependence of heterotypic ZfCx45-MCx45 junctions. These heterotypic junctions

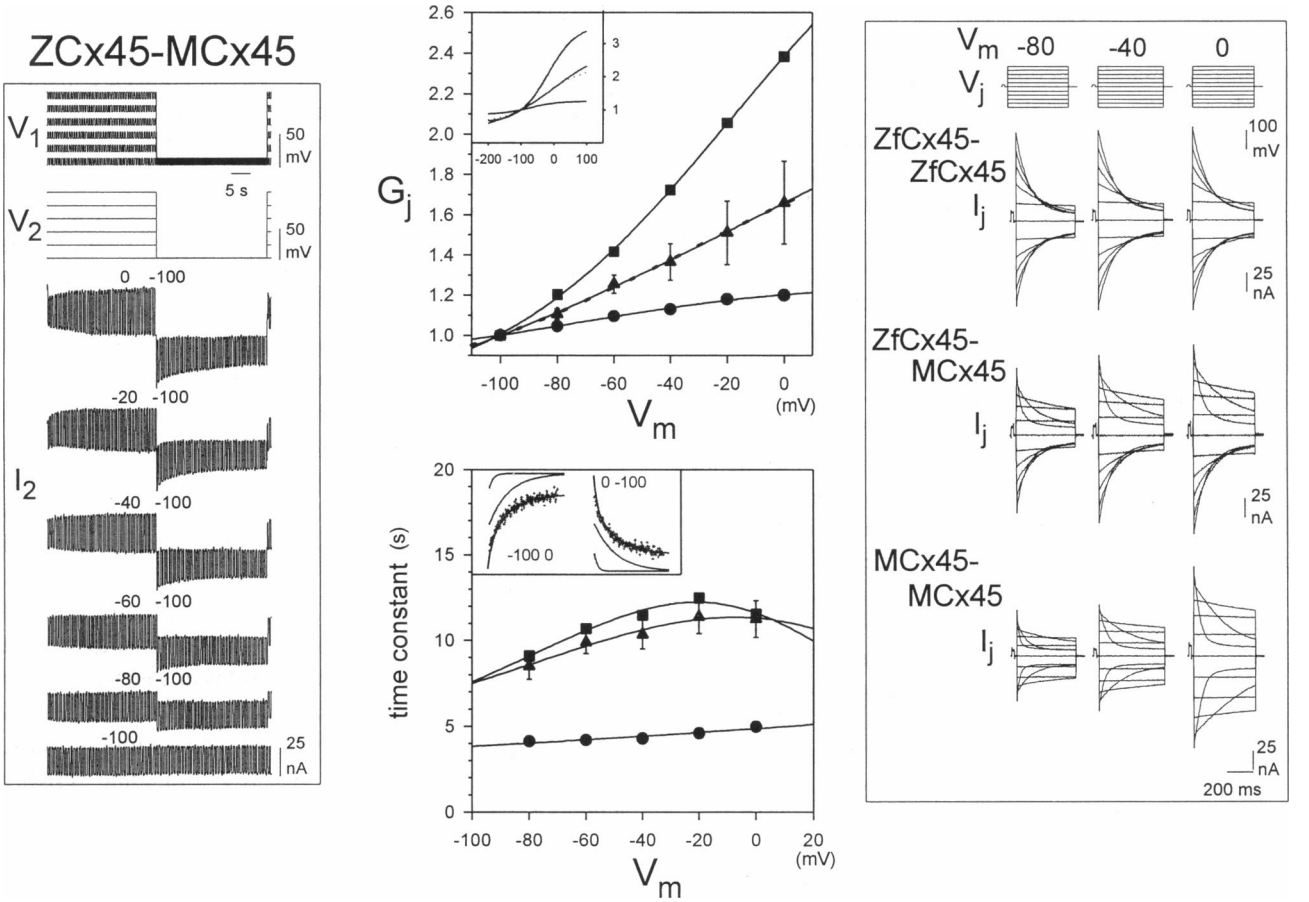

FIGURE 6 Inside-outside voltage dependence of heterotypic ZfCx45-MCx45 junctions. (*Left*) Sample records of nonjunctional and junctional currents (I_2) induced by equal displacement of holding potentials in both cells of a pair, as in Fig. 4. g_j increased with increasing depolarization and decreased to the control value when V_m was returned to −100 mV. (*Upper middle*) Graph of steady-state G_j/V_m relations (mean ± SD, n = 6 pairs) of hybrid ZfCx45-MCx45 (▲) channels and homotypic ZfCx45 (●) and MCx45 (■) junctions; g_j normalized to the value at V_m = −100 mV. The continuous curves (*inset*) represent the fits to squared Boltzmann relations of homotypic ZfCx45 and MCx45 junctions and the theoretical curve of hybrid ZfCx45-MCx45 calculated as the product of two single Boltzmann relations, with those parameters obtained for MCx45 and ZfCx45 hemichannels in their homotypic junctions (Table 1). The V_m dependence of heterotypic junctions was intermediate to those exhibited by parent homotypic junctions and was well described by that calculated to each hemichannel of homotypic MCx45 junction (*discontinuous curves*). (*Bottom*) Dependence of time constants on V_m. Time courses of increasing and decreasing g_j were well fitted by biexponential relations (*inset*) with a fast component of minor amplitude and a main component of slower kinetics. The calculated time constants for the major component of hybrid junctions (▲) plotted as a function of V_m, and those from homotypic MCx45 (■) and ZfCx45 (●) junctions superimposed. In the hybrid junctions, the time constants of the main component were close to those of homomeric MCx45 channels. (*Right*) Independence of V_m and V_j actions. Junctional currents of homotypic and heterotypic ZfCx45 and MCx45 junctions in response to the same transjunctional voltage protocols (V_j = ±100 mV, increments 20 mV, duration 500 ms) applied at three V_m levels (*left*, −80 mV; *middle*, −40 mV; *right*, 0 mV). At more depolarized V_m levels, g_j of the ZfCx45-ZfCx45 pair increased slightly, that of the MCx45-MCx45 pair markedly, and that of the ZfCx45-MCx45 pair moderately.

combine ZfCx45 hemichannels, which showed little effect of V_m, with MCx45 hemichannels, which are strongly V_m sensitive in the parental homomeric junctions. Equal depolarization of both sides of heterotypic ZfCx45-MCx45 junctions increased g_j in the same way that it increased g_j in homomeric ZfCx45 and MCx45 junctions (Fig. 4 and Fig. 6, *left*). The steady-state G_j/V_m relationships of ZfCx45-MCx45 junctions showed that the V_m influence was intermediate between those on their respective ZfCx45 and MCx45 homotypic junctions (Fig. 6, *middle upper graph*). The G_j/V_m relation could be fitted to the product of the single Boltzmann with the fitting parameters of squared relations used to describe the behavior of homotypic MCx45 and ZfCx45 junctions, supporting the assumption of a model of two independent gates in series (Table 2). The kinetic data from heterotypic junctions were also in agreement with this model. The time courses of the increasing and decreasing g_j transitions for depolarizing and hyperpolarizing membrane potential changes followed biexponential time courses with an initial fast component of minor amplitude and a main component of slower time constants. They varied as a function of V_m values in a way similar to those previously determined in the case of the homomeric ZfCx45 and MCx45 junctions, respectively (Fig. 6, *middle bottom*). Because voltage sensitivity and the kinetic properties exhibited by the ZfCx45-MCx45 junctions over-

lapped those observed in the homomeric MCx45 and ZfCx45 junctions, the V_m dependence of the hybrid junctions may be mainly accounted for by MCx45 hemichannels, whereas the contribution of the ZfCx45 hemichannel was negligible. This may suggest the existence of a specific V_m gate localized in each hemichannel that retained all gating characteristics presented by the homomeric combinations.

Finally, we examined interactions between V_j and V_m in gating Cx45 junctions. The same transjunctional voltages ($\pm$100 mV, 500 ms) were applied at three V_m levels (−80, −40, and 0 mV) in pairs expressing homotypic and heterotypic ZfCx45 and MCx45 junctions (Fig. 6, *right*). As described above, depolarizing V_m from −80 to 0 mV only slightly increased the g_j of homotypic ZfCx45 junctions, whereas it increased the g_j of homotypic MCx45 junctions 2.5-fold. Interestingly, reductions in g_j induced by positive and negative V_j steps were roughly symmetrical and had similar kinetics, although the V_j steps necessarily altered V_m in one cell of the pair. The normalized initial and steady-state g_j/V_j relations obtained at the three V_m levels superimposed almost perfectly (plots not shown). Both features indicated that the characteristics of V_j dependence were not modified by V_m. Note that when long V_j pulses with durations in the range of time constants of V_m dependence were used (see Fig. 2), neither acted asymmetrically. Similarly, in the case of MCx45-ZfCx45 heterotypic junctions, the junctional conductance responded to V_j with the same characteristic asymmetry at all three V_m levels. The apparent absence of an effect of V_m on V_j-induced changes in g_j suggests that the two types of voltage may regulate the junctional conductance through specific voltage sensors and with distinct gating mechanisms.

DISCUSSION

Species-specific voltage-gating properties

The first conclusion from this study is that analogous Cx45 subunits from four species form cell-to-cell channels with unique voltage-gating phenotypes. Although they have V_j and V_m sensitivity in common, there were striking differences in their voltage sensitivities and kinetics in response to both types of electrical fields.

The macroscopic junctional conductances of zebrafish, chicken, mouse, and human Cx45 junctions were strongly dependent on V_j. The g_j reductions were detectable, even at small V_j, and the g_j decreased to very low values at larger V_j. Furthermore, Cx45 junctions combined the marked voltage sensitivity with small values of V_0, the voltage for half-inactivation of g_j (10–30 mV), and fast kinetics of closing. Taken together, these data indicate that the subfamily of Cx45 junctions is among those intercellular junctions that show the most pronounced V_j dependence, jointly with *Xenopus* Cx38 (Ebihara et al., 1989); rodent and human Cx37 (Willecke et al., 1991; Reed et al., 1993); rat Cx40 (Bruzzone et al., 1993) and its homolog in chicken, Cx42 (Barrio et al., 1995b); and mouse Cx50 (White et al., 1992) and the counterpart in avian, chicken Cx45.6 (Jiang et al., 1994). In teleost, the zebrafish Cx45 junctions are markedly more V_j sensitive than the Cx32.2 junctions, recently cloned from the ovary of the Atlantic croaker (Bruzzone et al., 1995).

The V_m dependence is also a differential regulatory property among the orthologous Cx45 junctions of four species. Although the g_j of all of the types of Cx45 junctions increased with the degree of depolarization, the influence of V_m varied among them. It was very small on ZfCx45 junctions and moderate on avian and more marked on mammalian junctions, MCx45 junctions being more sensitive than HCx45 junctions. Moreover, the first-order kinetics of g_j transitions were slow with time constants of seconds that also varied among junctions of different species. Gap junctions with a combined V_j and V_m sensitivity were initially described in several junctions of insects (Verselis et al., 1991; Bukauskas et al., 1992; Churchill and Caveney, 1993). V_m dependence in these cases was characterized by being highly voltage sensitive with faster kinetics and by a complete block of junctional conductance in response to depolarizations in the physiological range. More recently, a weaker V_m dependence was also found in some vertebrate junctions. Thus the g_j of rat Cx26, like that of Cx45 junctions, increased with depolarization (Barrio et al., 1991). In contrast, the g_j of other vertebrate junctions, including Cx43 of *Xenopus*, chicken, rat, and human (Barrio et al., 1993, 1995a; White et al., 1994) and *Xenopus* Cx30 (Jarillo et al., 1995), is increased by hyperpolarization.

Species specificity of V_j and V_m dependence of gap junctions formed by orthologous connexins has also been observed in other instances. Human Cx43 and chicken Cx43 junctions expressed in transfected cells differ in their V_j dependence (Fishman et al., 1991; Veenstra et al., 1992), and the *Xenopus*, chicken, rat, and human Cx43 junctions studied in pairs of *Xenopus* oocytes showed striking differences with regard to their V_j and V_m dependencies (Barrio et al., 1995a). Mouse Cx37 expressed in oocytes exhibits a two-component decrease in g_j in response to V_j (Willecke et al., 1991), whereas changes in g_j of human Cx37 expressed in transfected cells are well described by a single Boltzmann relation (Reed et al., 1993). When rat Cx32 and its homolog in *Xenopus*, Cx30, are both expressed in paired oocytes, they exhibited quite different V_j and V_m gating properties (Jarillo et al., 1995). Finally, the orthologs rat Cx46, bovine Cx44, and chicken Cx56 formed functional hemichannels and complete junctional channels with divergent gating properties (Gupta et al., 1994; Ebihara et al., 1995; Trexler et al., 1996). Thus a major conclusion here is the existence of species specificity between orthologous junctions with respect to their voltage gating. Similarly, species-specific functional diversity may involve other types of regulatory gatings, such as by rises in cytoplasmic H^+ or Ca^{2+} concentration.

Voltage-gating model of Cx45 channels with separate V_j and V_m gates

The junctional conductance of the four species of Cx45 junctions showed a characteristic voltage dependence with sensitivity to both V_j and V_m. This complex voltage regulation could be explained by a unique gate capable of responding to V_m and V_j or by the existence of two different gates, each of them specifically sensing one type of voltage. The hypothesis of two separated gates is supported by 1) the striking differences in voltage sensitivity and the kinetics of responses to V_j and V_m (compare Figs. 2 and 3 with 4); 2) the absence of an obvious interaction between V_j and V_m effects on g_j when V_j pulses were applied (Figs. 1 and 6), although application of V_j must change V_m in one cell; and 3) the independent and divergent evolution of gating properties attributable to each kind of voltage among fish, avian, and mammalian Cx45 junctions. Additional evidence in favor of two separate gates localized into each hemichannel is the voltage-gating properties exhibited by the hybrid ZfCx45-MCx45 junctions (Figs. 5 and 6), because ZfCx45 and MCx45 hemichannels largely retained the V_m and V_j gating properties attributable to each kind of hemichannel in their corresponding parent homotypic channels. Taken together, the complete channel must contain at least four gates—two controlled by V_j and two controlled by V_m. The V_m sensor is weakly voltage sensitive and operates through a gating mechanism with slow (seconds) first-order kinetics. A comparison of the V_m sensitivity exhibited by g_j of hybrid ZfCx45-MCx45 junctions with those of the corresponding homotypic junctions suggests that V_m gates of the two hemichannels act independently (Figs. 4 and 6).

The V_j relatively negative on the cytoplasmic side of Cx45 hemichannels tends to reduce junctional conductance with a complex kinetics exhibiting sequentially three components: 1) an initial rectification of minor amplitude that was observed in avian and mammalian but not in zebrafish Cx45 junctions; 2) a major component of g_j decay with fast but resolvable kinetics; and 3) a minor component with slower kinetics only detectable at higher V_j (>50–60 mV). The initial rectification may correspond to a gate with very fast kinetics, faster than our clamping time resolution, or, alternatively, may represent single-channel rectification, as has been reported in rat Cx46 hemichannels (Trexler et al., 1996) and rat heterotypic Cx32-Cx26 channels (Bukauskas et al., 1995). The fast and more voltage-sensitive component of the decrease in g_j decay may reflect transitions between the fully open state and a substate, as has been reported for chicken Cx45 channels (Veenstra et al., 1994a) and human Cx45 channels (Moreno et al., 1995). The additional slower g_j reduction at larger voltages may represent transitions between substate and the fully closed state. A similar model of junctional channels with sensitivity to both V_j and V_m was proposed previously for insect gap junctions (Bukauskas and Weingart, 1994). These junctional channels operate with fast transitions between several open conductance substates under V_j control and with slower transitions between residual to closed states induced by depolarization of V_m.

Structure-function correlations of voltage-gating phenotypes

An overall correlation can be seen between the V_j and V_m gating phenotypes among four species of Cx45 channels and the degree of identity of their amino acid sequences. Thus the avian, mouse, and human Cx45 channels, which show more similar gating phenotypes, also show greater identity in their primary amino acid sequences (Fig. 1, *left*). Mouse and human Cx45 are 97% identical, with only 11 amino acid substitutions, five of which are conservative, and no deletions or insertions. The identity between avian and mammalian Cx45 is still very high (83%), with 56 substitutions (five conservative), five insertions, and three deletions. In contrast, the zebrafish Cx45 shows only 52–54% identity with the other Cx45s and exhibits the most divergent voltage gating phenotype. This correlation between voltage gating phenotype and the molecular distance on the Cx45 phylogenetic tree, generated from analysis of the divergence of amino acid sequences, is in agreement with vertebrate evolution inferred from other genotypic, phenotypic, and paleontological evidence (Løvtrup, 1977).

The divergences between mammalian, bird, and fish Cx45 amino acid sequences are not distributed uniformly throughout the topological domains of molecule (Fig. 1, *right*). In accordance with the general topology of connexins predicted by the hydropathy plots, which has been supported by antibody and protease studies (Bennett et al., 1991), there are nine principal domains: four membrane-spanning regions (M1–M4); two extracellular loops (E1, E2); a cytoplasmic loop (CL) connecting M2 and M3; and the amino terminus (NT) and carboxy terminus (CT) in the cytoplasmic side. The main differences among primary sequences of Cx45 from the four species are localized in a major part of the cytoplasmic loop and most of the carboxyl-terminal, which are also the most variable regions among other genes of the connexin family that have evolved in parallel, i.e., evolutionary paralogs (Bennett et al., 1995). On the other hand, there are domains and residues that are highly conserved in Cx45 from the four species. Some interesting insights into the molecular basis of voltage gating can be deduced by examination of the primary sequences and comparison of the common and divergent features of the four Cx45 gating phenotypes and of those of junctions formed by other connexins. The four kinds of Cx45 channels close with the negative polarity of V_j on the cytoplasmic side, the same polarity of closure as seen in rat Cx32 channels (Verselis et al., 1994). Accordingly, all four types of Cx45 contain the same motif of charged residues, which is proposed to be an integral part of the transjunctional voltage sensor of Cx32 channels, i.e., a neutral residue in the second or third position of the amino terminal, and Glu and Ser at the M1/E1 border (Verselis et al., 1994).

Thus these charged residues found in Cx32 predict the gating polarity of the four types of Cx45. Furthermore, in avian and mammalian Cx45 channels, this motif accounts for the calculated gating charge (n = 2.0), which is similar to that found in rat Cx32 channels. However, the larger calculated gating charge of ZfCx45 channels (n = 4.9) suggests that other charged residues may form part of the voltage sensor. Other differences in V_j dependence, such as the shifted G_{jss}/V_j relations and the differences in kinetics between chicken, mouse, and human Cx45 channels in the absence of changes in the gating charge, may reflect differences in the free energies of the open and closed states and the height of the energy barrier between them.

An original contribution of this work is the evidence for a V_m gate intrinsic to the hemichannel, as has previously been proposed for the V_j gate. Further studies involving site-directed mutagenesis will be required to identify the residues that comprise the V_m sensor.

Functional role of V_m and V_j dependencies

The voltage gating of gap-junctional channels provides a rapid control of cell-to-cell coupling. The strong V_j dependence exhibited by zebrafish, chick, mouse, and human Cx45 channels, defined by a large voltage-sensitive component (>90%) with a relatively low half-inactivation voltage (10–30 mV) and fast kinetics, makes this gating an attractive mechanism for mediating transitions between coupling and uncoupling. This is particularly true in poorly coupled cells in which cell-to-cell voltage gradients can be created easily, as has been established previously for junctions between amphibian blastomeres (Harris et al., 1983), the voltage dependence of which is similar to that of Cx45 channels. In avian and mammalian Cx45 channels, V_m dependence is great enough that intercellular coupling could be directly regulated by membrane potential, a stimulus always present and possibly varying, especially in excitable cells such as myocardiocytes, which express Cx45 in chicken, mouse, and human (Beyer, 1990; Hennemann et al., 1992; Kanter et al., 1994). Interestingly, V_m gating may regulate the degree of coupling independently and in the absence of V_j. The physiological role and functional significance of voltage dependence mediated by Cx45 junctions must be determined in adult tissues, as well as during development, when higher levels of Cx45 are expressed in all of the species studied so far (Beyer, 1990; Hennemann et al., 1992; Kanter et al., 1994; Essner et al., 1996).

We thank Prof. Daniel Gros, Prof. Klaus Willecke, and Prof. Eric Beyer for supplying the zebrafish, mouse, and chicken and human Cx45 cDNAs, respectively. We are grateful to Prof. M. V. L. Bennett for his critical reading of the manuscript. Mrs. Rosa Barquero carried out all of the technical assistance with oocytes.

This work was supported by a Fondo de Investigaciones Sanitarias grant (95/0643) to LCB, and an EC contract (BMH4-CT96-1427).

REFERENCES

Barrio, L. C., A. Handler, and M. V. L. Bennett. 1993. Inside-ouside and transjunctional voltage dependence of rat connexin43 expressed in pairs of *Xenopus* oocytes. *Biophys. J.* 64:A191. (Abstr.)

Barrio, L. C., J. A. Jarillo, and C. Castro. 1995a. Connexin 43 channels from different species have divergent regulation by voltage but all share the same polarity of closure. *In* Proceedings of the 1995 Gap Junction Conference. L'Ile des Embioz, France.

Barrio, L. C., J. A. Jarillo, J. C. Sáez, and E. C. Beyer. 1995b. Comparison of voltage dependence of chick connexin 45 and 42 channels expressed in pairs of *Xenopus* oocytes. *In* Gap Junctions. Y. Kanno, editor. Progress in Cell Research, Vol. 4. Elvesier Science, Amsterdam. 391–394.

Barrio, L. C., T. Suchyna, T. Bargiello, L. X. Xu, R. S. Roginski, M. V. L. Bennett, and B. J. Nicholson. 1991. Gap junctions formed by connexins 26 and 32 alone and in combination are differently affected by applied voltage. *Proc. Natl. Acad. Sci. USA.* 88:8410–8414.

Beblo, D. A., H-Z. Wang, E. C. Beyer, E. M. Westphale, and R. D. Veenstra. 1995. Unique conductance, gating, and selective permeability properties of gap junction channels formed by connexin-40. *Circ. Res.* 77:813–822.

Bennett, M. V. L., L. C. Barrio, T. A. Bargiello, D. C. Spray, E. Hertzberg, and J. C. Sáez. 1991. Gap junctions: new tools, new answers, new questions. *Neuron.* 6:305–320.

Bennett, M. V. L., and V. K. Verselis. 1992. Biophysics of gap junctions. *Semin. Cell Biol.* 3:29–47.

Bennett, M. V. L., X. Zheng, and M. L. Sogin. 1995. The connexin family tree. *In* Gap Junctions. Progress in Cell Research, Vol. 4. Y. Kanno, K. Kataoka, Y. Shiba, Y. Shibata, and T. Shimazu, editors. Elvesier, Amsterdam. 3–8.

Beyer, E. C. 1990. Molecular cloning and developmental expression of two embryo gap junction proteins. *J. Biol. Chem.* 265:14439–14443.

Bruzzone, R., J-A. Hefliger, R. L. Gimlich, and D. L. Paul. 1993. Connexin40, a component of vascular endothelium, is restricted in its ability to interact with other connexins. *Mol. Biol. Cell.* 4:7–20.

Bruzzone, R., T. W. White, and D. L. Paul. 1996. Connections with connexins: the molecular basis of direct intercellular signaling. *Eur. J. Biochem.* 238:1–27.

Bruzzone, R., T. W. White, G. Yoshizaki, R. Patiño, and D. L. Paul. 1995. Intercellular channels in teleosts: functional characterization of two connexins from Atlantic croaker. *FEBS Lett.* 358:301–304.

Bukauskas, F. F., C. Elgang, K. Willecke, and W. Weingart. 1995. Heterotypic gap junction channels (connexin26-connexin32) violate the paradigm of unitary conductance. *Pflügers Arch. Eur. J. Physiol.* 429: 870–872.

Bukauskas, F. F., C. Kempf, and R. Weingart. 1992. Electrical coupling between cells of the insect *Aedes Albopicus. J. Physiol. (Lond.).* 448: 321–337.

Bukauskas, F. F., and R. Weingart. 1994. Voltage-dependent gating of single gap junction channels in an insect cell line. *Biophys. J.* 67: 613–625.

Chen, S-C., L. M. Davis, E. M. Westphale, E. R. Beyer, and J. E. Saffitz. 1994. Expression of multiple gap junction proteins in human fetal and infant hearts. *Pediatr. Res.* 36:561–566.

Churchill, D., and S. Caveney. 1993. Double whole-cell patch-clamp characterization of gap junctional channels in isolated insect epidermal cell pairs. *J. Membr. Biol.* 135:165–180.

Ebihara, L., E. C. Beyer, K. I., Swenson, D. L. Paul, and D. A. Goodenough. 1989. Cloning and expression of a *Xenopus* embryonic gap junction. *Science.* 243:1194–1195.

Ebihara, L., V. M. Berthoud, and E. C. Beyer. 1995. Distinct behavior of connexin56 and connexin46 gap junctional channels can be predicted from the behavior of their hemi-gap-junctional channels. *Biophys. J.* 68:1796–1803.

Elfgang, C., R. Eckert, H. Lichtenberg-Fraté, A. Butterweck, O. Traub, R. A. Klein, D. L. Hülser, and K. Willecke. 1995. Specific permeability and selective formation of gap junction channels in connexin-transfected HeLa cells. *J. Cell Biol.* 129:805–817.

Essner, J. J., J. G. Laing, E. C. Beyer, R. G. Johnson, and P. B. Hackett. 1996. Expression of zebrafish connexin43.4 in the notochord and tail bud of wild-type and mutant no tail embryos. *Dev. Biol.* 177:449–462.

Fishman, G., A. P. Moreno, D. C. Spray, and L. A. Leinwand. 1991. Functional analysis of human cardiac gap junction channel mutants. *Proc. Natl. Acad. Sci. USA.* 88:3525–3529.

Gupta, V. K., V. M. Berthoud, N. Atal, J. A. Jarillo, L. C. Barrio, and E. C. Beyer. 1994. Bovine connexin44, a lens gap junction protein: molecular cloning, immunological characterization and functional expression. *Invest. Ophthalmol. Vis. Sci.* 35:3747–3758.

Harris, A., D. C. Spray, and M. V. L. Bennett. 1981. Kinetic properties of a voltage-dependent junctional conductance. *J. Gen. Physiol.* 77: 95–117.

Harris, A., D. C. Spray, and M. V. L. Bennett. 1983. Control of intercellular communication by voltage dependence of gap junctional conductance. *J. Neurosci.* 3:79–100.

Hennemann, H., H. J. Schwarz, and K. Willicke. 1992. Characterization of gap junction genes expressed in F9 embryonic carcinoma cells: molecular cloning of mouse connexin31 and -45 cDNAs. *Eur. J. Cell Biol.* 57:51–58.

Hermans, M. M. P., P. Kortekaas, H. J. Jongsma, and M. B. Rook. 1995. pH sensitivity of the cardiac gap junction proteins, connexin45 and 43. *Pflügers Arch. Eur. J. Physiol.* 431:138–140.

Higgins, D. G., and P. M. Sharp. 1988. Clustal: a package for performing multiple sequence alignments on a microcomputer. *Gene.* 73:237–244.

Jarillo, J., L. C. Barrio, and R. L. Gimlich. 1995. Voltage dependence and kinetics of *Xenopus* connexin 30 channels expressed in *Xenopus* oocytes. *In* Gap Junctions. Progress in Cell Research, Vol. 4. Y. Kanno, editor. Elsevier Science, Amsterdam. 399–402.

Jiang, J. X., T. W. White, D. A. Goodenough, and D. L. Paul. 1994. Molecular cloning and functional characterization of chick lens fiber connexin-45.6. *Mol. Biol. Cell.* 5:363–373.

Kanter, H. L., J. G. Laing, E. C. Beyer, K. G. Green, and J. E. Saffitz. 1993. Multiple connexins colocalize in canine ventricular myocyte junctions. *Circ. Res.* 73:344–350.

Kanter, H. L., J. E. Saffitz, and E. C. Beyer. 1992. Cardiac myocytes express multiple gap junction proteins. *Circ. Res.* 70:438–444.

Kanter, H. L., J. E. Saffitz, and E. C. Beyer. 1994. Molecular cloning of two human gap junction proteins, connexin40 and connexin45. *J. Mol. Cell Cardiol.* 26:861–868.

Liu, S., S. Taffet, L. Stoner, M. Delmar, M. L. Vallano, and J. Jalife. 1993. A structural basis for the unequal sensitivity of the major cardiac and liver gap junctions to intracellular acidification: the carboxyl tail length. *Biophys. J.* 64:1422–1433.

Løvtrup, S. 1977. The Phylogeny of Vertebrates. John Wiley and Sons, New York.

Moreno, A. P., J. G. James, E. C. Beyer, and D. C. Spray. 1995. Properties of gap junction channels formed of connexin45 endogenously expressed in human hepatoma (SKHep1) cells. *Am. J. Physiol.* 268:C356–C365.

Moreno, A. P., M. B. Rook, G. I. Fishman, and D. C. Spray. 1994. Gap junction channels: distinct voltage-sensitive and insensitive conductance states. *Biophys. J.* 67:113–119.

Nicholson, B. J., T. Suchyna, L. X. Xu, P. Hammernick, F. L. Cao, C. Fourtner, and L. C. Barrio, and M. V. L. Bennett. 1993. Divergent properties of different connexins expressed in *Xenopus* oocytes. *In* Gap Junctions. Progress in Cell Research, Vol. 3. J. E. Hall, G. A. Zampighi, and R. M. Davis, editors. Elsevier, Amsterdam. 3–13.

Reed, K. E., E. M. Westphale, D. M. Larson, H-Z. Wang, R. D. Veenstra, and E. C. Beyer. 1993. Molecular cloning and functional expression of human connexin37, an endothelial cell gap junction protein. *J. Clin. Invest.* 91:997–1004.

Spray, D. C., A. L. Harris, and M. V. L. Bennett. 1981. Equilibrium properties of a voltage-dependent junctional conductance. *J. Gen. Physiol.* 77:77–93.

Steiner, E., and L. Ebihara. 1996. Functional characterization of canine connexin45. *J. Membr. Biol.* 150:153–161.

Trexler, E. D., M. V. L. Bennett, T. A. Bargiello, and V. K. Verselis. 1996. Voltage gating and permeation in a gap junction hemichannel. *Proc. Natl. Acad. Sci. USA.* 93:5836–5841.

Veenstra, J. D., H. Z. Wang, E. M. Westphale, and E. C. Beyer. 1992. Multiple connexins confer distinct regulatory and conductance properties of gap junctions in developing heart. *Circ. Res.* 71:1277–1283.

Veenstra, R. D., H-Z. Wang, E. C. Beyer, and P. R. Brink. 1994a. Selective dye and ionic permeability of gap junction channels formed by connexin45. *Circ. Res.* 75:483–490.

Veenstra, R. D., H-Z. Wang, E. C. Beyer, S. V. Ramanan, and P. R. Brink. 1994b. Connexin37 forms high conductance gap junction channels with subconductances state activity and selective dye and ionic permeabilities. *Biophys. J.* 66:1915–1928.

Verselis, V. K., M. V. L. Bennett, and T. A. Bargiello. 1991. A voltage-dependent gap junction in *Drosophila melanogaster*. *Biophys. J.* 59: 114–126.

Verselis, V. K., C. S. Ginter, and T. A. Bargiello. 1994. Opposite voltage gating polarities of two closely related connexins. *Nature.* 368:348–351.

Werner, R., E. Levine, C. Rabadan-Diehl, and G. Dahl. 1989. Formation of hybrid cell-to-cell channels. *Proc. Natl. Acad. Sci. USA.* 86:5380–5384.

White, T. W., R. Bruzzone, D. A. Goodenough, and D. L. Paul. 1992. Mouse Cx50, a functional member of the connexin family of gap junction proteins, is the lens fiber protein MP70. *Mol. Biol. Cell.* 3:711–720.

White, T. W., R. Bruzzone, and D. L. Paul. 1995. The connexin family of intercellular forming proteins. *Kidney Int.* 48:1148–1157.

White, T. W., R. Bruzzone, S. Wolfram, D. L. Paul, and D. A. Goodenough. 1994. Selective interactions among the multiple connexin proteins expressed in the vertebrate lens: the second extracellular domain is a determinant of compatibility between connexins. *J. Cell Biol.* 125: 879–892.

Wilders, R., and H. J. Jongsma. 1992. Limitations of the dual voltage clamp method in assaying conductance and kinetics of gap junction channels. *Biophys. J.* 63:942–953.

Willecke, K., R. Heynkes, E. Dahl, R. Stutenkemper, H. Hennemann, S. Jungbluth, T. Suchyna, and B. J. Nicholson. 1991. Mouse connexin37: cloning and functional expression of a gap junction gene highly expressed in lung. *J. Cell Biol.* 114:1049–1057.